Research Article

Qizhi Luo, Yu-You Wu*, Wenjun Qiu, Haoliang Huang, Songfeng Pei, Paul Lambert, and David Hui

Improving flexural strength of UHPC with sustainably synthesized graphene oxide

https://doi.org/10.1515/ntrev-2021-0050
received June 22, 2021; accepted July 16, 2021

Abstract: Ultrahigh-performance concrete (UHPC) has been increasingly employed for infrastructure and building structure, thanks to its excellent durability and exceptional mechanical properties; however, improving its relatively low flexural strength remains a challenging issue. This study presents an experimental investigation on improving the compressive strength and flexural strength of UHPC by employing sustainably synthesized graphene oxide (GO). The content of micro steel fibers (MSFs) for the UHPC ranges from 0.5 to 1.5% by volume of concrete. For each level of MSFs addition, the dosage of GO added is from 0.00 to 0.03% by mass of cement. The results indicate that the electrochemical (EC) method to synthesize GO is greener, safer, and lower in cost for construction industry. And the compressive strength of UHPC is slightly improved, while its flexural strength is significantly increased from 33 to 65%, demonstrating that the incorporation of GO can be an effective measure to enhance the flexural strength of UHPC under standard curing and steam curing. This can be associated with the improvement in bond strength between the MSFs and the matrix contributed by the improved interfacial microstructure, the higher friction increase, and the mechanical interlock at the interface between the MSFs and the bulk matrix, thanks to the addition of GO.

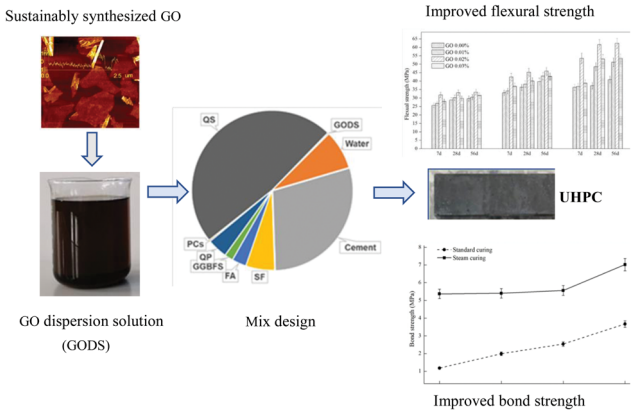

Graphical abstract

Keywords: sustainably synthesized graphene oxide, ultrahigh-performance concrete, flexural strength

1 Introduction

Ultrahigh-performance concrete (UHPC) has been increasingly employed for infrastructure and building structure, thanks to its exceptional mechanical properties and excellent durability [1,2]. Such superior performance is normally associated with factors such as the low water-to-binder ratio (w/b) and high particle packing density [3]; however, improving its relatively low tensile and flexural strengths remain a challenging issue.

Many attempts have been made to improve such properties of UHPC. The micro steel fibers (MSFs) play a critical role in improving its tensile and flexural performance, which is subject to the fiber shape, aspect ratio, fraction volume, fiber orientation and distribution, and the bond between the fiber and the cementitious matrix within UHPC matrix [4–11]. Meng and Khayat [12] reported

* **Corresponding author: Yu-You Wu,** School of Transportation, Civil Engineering and Architecture, Foshan University, Foshan 528225, Guangdong, China, e-mail: yuyou.wu@yahoo.com
Qizhi Luo: School of Transportation, Civil Engineering and Architecture, Foshan University, Foshan 528225, Guangdong, China
Wenjun Qiu: Foshan Transportation Science and Technology Ltd, Guangzhou 528300, Guangdong, China.
Haoliang Huang: School of Materials Science and Engineering, South China University of Technology, Guangzhou 510640, Guangdong, China
Songfeng Pei: Shenyang National Laboratory for Materials Science, Institute of Metal Research, Chinese Academy of Sciences, Shenyang 110016, China
Paul Lambert: Materials and Engineering Research Institute, Sheffield Hallam University, Sheffield, S1 1WB, United Kingdom
David Hui: Department of Mechanical Engineering, University of New Orleans, New Orleans, LA 70148, United States of America

that the greatest steel fiber dispersion uniformity and optimum flexural property of UHPC can be obtained by managing the rheology of the mortar. And the results indicated that with a w/b of 0.23, 2% of MSF by volume, and 1% of viscosity modified admixture, the 28 days compressive and flexural strengths are approximately 120 and 35 MPa, respectively, demonstrating that the flexural strength was increased by 42%. Huang *et al.* [13] developed an L-shaped device to control the flow of fresh mixture to improve the orientation of MSFs within UHPC matrix and the results indicated that with 2% of MSF and a w/b of 0.20 under steam curing, its compressive and flexural strengths are about 150 and 40 MPa, respectively, with the flexural strength increased by 33% compared to unorientated fibers after exposure to elevated temperature. The authors also observed that such values of these strengths with the same content of MSF and a w/b of 0.22 are approaching 140 and 35 MPa, demonstrating that the flexural strength was increased by 35% compared to samples with unorientated fibers.

Nanomaterials (*e.g.*, nano-SiO_2, carbon nanotube, carbon nanofiber, graphite nanoplatelet [GNP], *etc.*) are all able to contribute to an enhancement in the mechanical properties [14,15]. Wu *et al.* [16] found that the addition of nano-SiO_2 can improve the compressive strength of UHPC and the interface bond strength between steel fiber and matrix. Such improvement was associated with lower porosity, denser, and more homogeneous microstructures of the matrix as well as the enhanced chemical bond of calcium–silicate–hydrate (C–S–H) of the fibers within the UHPC. Unlike nano-SiO_2, carbon-based nanomaterials (*e.g.*, carbon nanotube, carbon nanofiber, GNP, and graphene oxide [GO]) have no chemical activity within cementitious composites. Wille and Loh [17] identified that the low concentrations of multiwalled carbon nanotubes greatly improved the interface bond performance between steel fibers and the concrete matrix. By incorporating carbon nanofibers, Meng and Khayat [18] observed that the compressive strength of UHPC with 0.5% of MSF and a w/b of 0.2 was slightly increased as the content went up from 0 to 0.30% by cementitious mass, while the 28 days tensile and flexural strengths were increased by 56 and 46%, respectively. The authors also confirmed that the compressive strength of such a UHPC incorporating GNP was greater than that of the one with carbon nanofibers, while the tensile strength, flexural strength, and the maximum force for single fiber pullout for UHPC containing GNP were enhanced by 40, 59, and 27%, respectively, when the dosage of GNP ranged from 0 to 0.30%. The results also indicated that UHPC with the addition of GNPs has a better flexural performance compared to the one with carbon nanofibers. This may be caused by the high tensile strength and the effects of nano size filler and bridging of the carbon nanofibers and GNP, thereby improving the microstructure of the matrix and the interface performance between the steel fibers and matrix [17,19].

Compared to carbon nanotube, carbon fiber, and GNP, GO is hydrophilic [20] and has been employed to improve the mechanical properties and durability of cement paste, mortar, and concrete [21–35]. More recently, advancements have been made in coupling GO with fiber to improve the properties of cement-based composites, predominantly the flexural performance. Jiang *et al.* [36] observed that the compressive and flexural strengths of mortar with the addition of both polyvinyl alcohol (PVA) fiber and GO at the age of 28 days was increased by 30.2 and 39.3%, respectively. These are associated with the promotion of cement hydration and refinement of the microstructure of the mortar. Yao *et al.* [37] chemically modified the PVA fiber-to-mortar interface by coating GO on the PVA fiber surface. The study results demonstrated that the addition of 0.5% of GO-coated PVA fibers by volume can improve the tensile strength of mortar by 36.0% when compared to that of a control sample with uncoated PVA fibers. The improvement was associated with the increase in the chemical bond energy at the interface between fiber and matrix. Lu *et al.* [38] developed a novel GO-coated polyethylene (PE) fiber to make it interact much more readily with cement hydrates. And the results indicated that the addition of 2.0% of GO-coated PE fiber-reinforced mortar can increase the tensile strength by 46.0% when compared to uncoated PE fibers. This notable improvement is considered to be mainly due to the strengthening of the PE fiber-to-matrix bond offered by the GO coating. This was verified by a single fiber pullout test suggesting an enhancement of interfacial bond strength from 2.33 to 3.99 MPa. As a result, GO may be considered a promising material for improving the properties of UHPC, especially its flexural performance. However, only limited investigation has been directed at such applications [39,40]. It is therefore desirable to further study and develop GO-based technology for UHPC applications in order to achieve enhanced performance, notably of its flexural strength.

This study presents an experimental investigation into improving the compressive and flexural strengths of UHPC by employing sustainably synthesized GO [41], which is considered to be safer, greener, and of lower cost compared to Hummer's method or the improved Hummer's method [21,42,43]. The levels of MSFs addition for

the UHPC are 0.5, 1.0, and 1.5% by volume of concrete. For each level of MSFs addition, the dosages of GO added are 0.00, 0.01, 0.02, and 0.03% by mass of cement. Flowability, compressive strength, and flexural strength of the UHPC are evaluated. A single fiber pullout test is carried out to evaluate the bond property between the fibers and the cementitious matrix and identify the reinforcing mechanism of GO for UHPC. Additionally, scanning electron microcopy (SEM) is employed to examine the microstructure of UHPC matrices and the fiber-to-matrix interfaces. The findings indicate that its compressive strength is slightly improved, while its flexural strength is significantly increased demonstrating that the incorporation of GO can be an effective measure to improve the flexural strength of UHPC under standard curing and steam curing.

2 Materials and experiments

2.1 Green synthesis and characterization of GO

The solution of GO was produced with a two-step EC method [41], which is a safer, greener, and lower in cost compared to Hummer's method or improved Hummer's method [21,42,43]. Commercially available flexible graphite paper (FGP) was used as raw material. First, the FGP was subjected to EC intercalation in the concentrated H_2SO_4 to form graphite intercalation compound paper which was then employed as the anode for the EC reaction in the diluted H_2SO_4 to achieve oxidation of the carbon lattice in the FGP to produce graphite oxide. After being vacuum filtrated and washed, filter cake was exfoliated in water by the sonication to form GO dispersion.

The SEM images of the GO sheets were obtained by means of a field emission electron gun FEI Nova Nano SEM 430, which was operated at 10.0 kV. The SEM samples were fabricated by dipping a silicon wafer (1 cm × 1 cm) into the GO solution with a concentration of 0.01 wt% and gradually withdrawing them from the solution allowing the GO sheets to stay on the surface of the silicon wafer slice. Then, the wafer sample was spray dried with N_2 gas. Atomic force microscope (AFM) images of the GO were obtained by means of a Bruker Dimension FastScan with ScanAsyst^{TM}, which was operated in the tapping mode. The compositions of the GO were evaluated on the freeze dried GO powder by means of an Elementar vario MICRO cube combustion elemental analyzer (EA).

2.2 Materials of UHPC

Ordinary Portland cement grade 42.5 (OPC 42.5) in accordance with GB/T 175-2007 [44], Class F fly ash (FA), ground granulated blast furnace slag (GGBFS), and silica fume (SF) were employed as binder materials for all mixtures of the UHPCs. Table 1 lists their chemical compositions and properties [39].

Quartz powder (QP) with an average diameter of 0.044 mm was employed for UHPC mixtures with high cement contents only. Quartz sand (QS) consisted of three grades QS1, QS2, and QS3. The corresponding diameter ranged from 0.212 to 0.425 mm, 0.425 to 0.85 mm, and 0.85 to 2.00 mm, respectively. The content of SiO_2 for both the QP and QS was greater than 99%. Straight MSF coated with copper and with a tensile strength of 2,800 MPa, length of 12–16 mm, and diameter of 0.18–0.25 mm was used. A polycarboxylate-based superplasticizer (PCs) was used and its water-reducing capacity was greater than 38%.

2.3 Mix proportions and preparation of UHPC specimens

The UHPC mixtures contained MSFs in the range of 0.5, 1.0, and 1.5% by volume of concrete. For each level of MSF addition, the dosage of GO added were from 0.00 to 0.03% by mass of cement. Table 2 lists the mix proportions of the UHPCs, based on the earlier study [45]. These mixtures had a w/b of 0.18 and a sand-to-binder volume ratio of 1.1. Water components consisted of the mixing water and GO water dispersion. The dosage of PCE was 0.3% by mass of binder materials.

For the mixing procedure, the GO water dispersion was diluted with potable water in a vessel and stirred at a speed of 2,000 rpm for few minutes. In parallel, the dried QS was mixed in a separate vessel for 1 min, followed by the addition of cementitious materials and PCE powder and mixed at a speed of 60 rpm for one more minute. The diluted GO dispersion was then added for mixing for 2 min. The MSF was stably added in over 1 min and mixed at a speed of 60 rpm. Finally, the mixing continued at a speed of 60 rpm for more than 3 min. Part of this mixture was sampled for the testing of flowability. The remaining mixture was cast into the molds that were pre-oiled. This was followed by being compacted on a vibration table which was electrically powered. After being covered with polyethylene sheets, these samples were cured in the laboratory environment for 24 h.

The specimens, with dimensions of 40 mm × 40 mm × 40 mm, were prepared for compressive strength tests,

Table 1: Compositions and properties of binder materials

Materials	Unit		OPC	SF	FA	GGBFS
SiO_2	wt%		21.00	95.30	53.97	42.00
Al_2O_3			5.40	1.20	31.15	16.00
Fe_2O_3			2.80	0.90	4.16	—
CaO			64.68	0.40	4.01	40.00
MgO			1.40	0.80	1.01	—
SO_3			2.19	—	0.73	1.72
K_2O				—	2.04	—
Na_2O				1.10	0.89	—
TiO_2				—	1.13	—
P_2O_5				—	0.67	—
Cl			0.01	—	0.13	0.05
NiO				—	0.11	—
Loss on ignition	g		2.52	0.30	—	0.23
Blaine surface area	m^2/kg		357.00	—	330.00	418.00
BET surface area			—	19500.00	—	—
Specific gravity			3140.00	2200.00	2280.00	2900.00
Setting time	min	Initial	203.00	—	—	—
		Final	250.00	—	—	—
Compressive strength	MPa	3 days	27.40	—	—	—
Flexural strength		3 days	5.90	—	—	—

while specimens with dimensions of 40 mm × 40 mm × 160 mm were prepared for flexural strength tests. As shown in Figure 1, dog-bone-shaped specimens for single fiber pullout test were prepared and the embedment depth of a 30 mm long steel fiber was 15 ± 2 mm. The dog-bone-shaped specimens were also employed to prepare samples for observation on the steel fiber-to-matrix interface by means of an SEM.

Two curing regimes were employed. After demolding, half of the specimens were cured at a temperature of 21 ± 2°C and a relative humidity greater than 95% until the age of testing, designated "standard curing." The remaining samples were moved into a steam box and cured with its temperature elevated to 90°C at a rate of 10°C per hour. It was held at 90°C for 24 h and then cooled to the room temperature at a rate of 10°C per hour, which was followed by further standard curing until the testing age, designated "steam curing."

2.4 Experimental procedure

2.4.1 Fresh property tests

Flow table tests were carried out to determine the rheology of UHPC according to ASTM C1437-15 [46]. For each test, the flow table was dropped for 20 times within approximately 20 s.

Table 2: Mix proportions of UHPC with high cement volume (kg/m^3)

MSF	GO	Water	Cement	SF	FA	GGBFS	QP	QS1	QS2	QS3	PCE
0.5%	0	190.02	703.8	140.8	70.4	42.2	98.5	504.9	363.5	292.8	3.167
	0.070	190.02	703.7	140.8	70.4	42.2	98.5	504.9	363.5	292.8	3.167
	0.141	190.02	703.6	140.8	70.4	42.2	98.5	504.9	363.5	292.8	3.167
	0.211	190.02	703.5	140.8	70.4	42.2	98.5	504.9	363.5	292.8	3.167
1.0%	0	186.84	692.0	138.4	69.2	41.5	96.8	496.4	357.4	287.9	3.114
	0.069	186.84	691.9	138.4	69.2	41.5	96.8	496.4	357.4	287.9	3.114
	0.138	186.84	691.8	138.4	69.2	41.5	96.8	496.4	357.4	287.9	3.114
	0.208	186.84	691.7	138.4	69.2	41.5	96.8	496.4	357.4	287.9	3.114
1.5%	0	184.74	680.5	136.1	68.0	40.8	95.2	488.2	351.5	283.1	3.062
	0.068	184.74	680.4	136.1	68.0	40.8	95.2	488.2	351.5	283.1	3.062
	0.136	184.74	680.3	136.1	68.0	40.8	95.2	488.2	351.5	283.1	3.062
	0.204	184.74	680.2	136.1	68.0	40.8	95.2	488.2	351.5	283.1	3.062

Figure 1: Specimens for single fiber pullout test.

After the fresh mixture reached the maximum extent of its flow, the average diameter was measured.

2.4.2 Mechanical performance tests

The compressive and flexural strengths of UHPC were tested at 7, 28, and 56 days. The tests were conducted by using MTS testing equipment in accordance with BS-EN-196-1 [47]. Each strength value listed was the average of six test results.

2.4.3 Single fiber pullout tests

Fiber pullout tests were performed by using testing equipment as illustrated in Figure 2 according to Chinese standard CECS13:2009 [48]. A displacement controlling method was applied for the test and the loading rates were 3 mm/min. The maximum pullout forces were recorded and the bond strength between steel fiber and the bulk matrix was calculated according to the maximum pullout force and the surface area of the embedded fiber. Each bond strength value listed was the average of six test results.

2.4.4 Microstructure characterization

The specimens at the age of 7 days were carefully cut along the direction perpendicular to the fiber. A cut surface of the samples was then ground with #120, #600, and #1500 abrasive papers and further polished with diamond polishing paste. During this process, anhydrous ethanol was used for flushing. The interface between the steel fibers and the bulk matrix of UHPC was examined by SEM. The backscattered electron (BSE) method was applied with an accelerating voltage of 20 kV and magnifications of 1,000×.

3 Results and discussions

3.1 Characteristic of GO

The GO was characterized by means of the AFM and the SEM. The GO monolayer showed a thickness of ~1.0 nm. Statistical analysis of the AFM images confirmed that the thickness distribution of GO was predominantly as monolayers (~91%), and all the GO were less than 3 layers, as illustrated in Figure 3a and b. The results obtained from the AFM and SEM measurements indicated that the lateral size of GO is mainly in the range of 0.5–3 μm (~80.3%), with ~2.7% larger than 3 μm and ~17 % smaller than 0.5 μm as shown in Figure 3c and d. The compositions of the GO were analyzed by means of the EA and the results showed that the GO had a mean C/O atomic ratio of ~1.67, suggesting a higher oxidation degree of GO. The GO compositions and dimensions are summarized in Table 3.

Prior to the present study, Hummer's method or the improved Hummer's method [21,42,43] had been most widely employed to synthesize GO for enhancing the properties of cement paste, mortar, and concrete [21]. However, this has resulted in significant concerns with regard to safety, negative environmental impact, and high cost because highly concentrated H_2SO_4 and $KMnO_4$ are used to ensure that the graphite is oxidized as completely as possible. Their reaction product, Mn_2O_7, is highly active and can explode at elevated temperature greater than 95°C. Moreover, a serious environmental pollution risk is associated with the high volume of wastewater containing mixed acids and metal ions when removing the H_2SO_4 and $KMnO_4$ following the oxidation reaction. In addition, it can take an extended time for the oxidation to complete, even when applying the strong oxidant K_2FeO_4 and concentrated H_2SO_4, further adding to the pollution risk. Clearly, it is not appropriate to employ Hummer's method or improved Hummer's method

Figure 2: Setup of single fiber pullout test.

to synthesize GO for large volume production as required by the construction industry. The EC method [41] for synthesizing exhibits a number of advantages, with H_2SO_4 being used principally as a fully recyclable control agent and without other oxidants which could otherwise contribute to explosion risks and the release of metal ion contamination. In addition, the oxidation rate of EC is relatively faster. Moreover, the cleaning of the produced graphite oxide needs less water. It is therefore apparent that the EC method to synthesize GO is potentially safer, greener, and of lower cost and should be suitable for fabricating GO for all cement-based composites such as cement paste, mortar, normal concrete, and high-performance concrete especially UHPC.

3.2 Fresh properties of UHPC with GO

Figure 4 shows the effect of MSF and GO on the flowability of the mixture. It can be seen that the combined effects of both GO and MSF have resulted in the reduction in the flowability of the mixture. When the content of GO is added from 0.0 to 0.03%, the flowability with an MSF of 0.5% is decreased from 221 to 186 mm, while with a 1% of MSF, the flowability is reduced from 197 to 176 mm. Similar trend is also observed on the UHPC with a 1.5% of MSF, where the flowability is reduced from 178 to 156 mm.

Previously it was reported that the decrease in concrete flowability due to GO might be attributed to its high specific surface area, causing the less availability of water to adequately wet the mixture [21]. It was also suggested that the flowability reduction in UHPC mixtures incorporating MSF may be associated with the increased specific surface area and random distribution of MSF [5]. It is therefore assumed that such combined factors have caused further decrease in flowability.

3.3 Compressive strength of UHPC influenced by GO

The compressive strength tested at 7, 28, and 56 days under standard curing is shown in Figure 5. For a given MSF content and a given age, it can be seen that the compressive strength is improved as the content of GO is increased compared to the reference specimens. It is also observed that for a given MSF content and a given age with additions of GO from 0 to 0.03%, the compressive strength of UHPC is first increased up to 0.02% but then stabilizes, indicating an optimal dosage of GO of around 0.02%. With this dosage, the corresponding

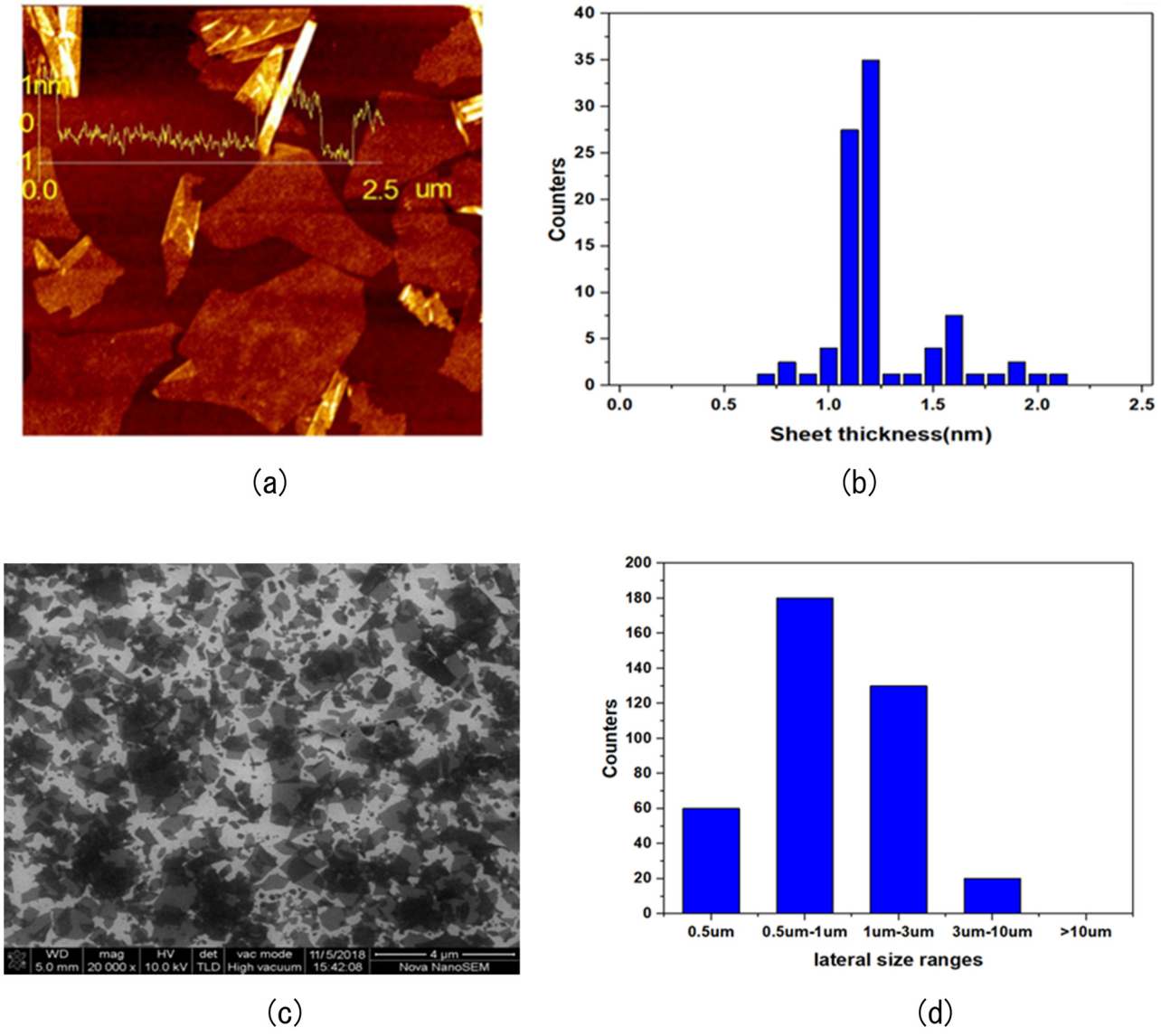

Figure 3: Characterization of GO. (a) typical AFM image of GO, (b) statistics of the thickness distribution of GO, (c) typical SEM image of GO, and (d) statistics of the lateral size distribution of GO.

Table 3: Compositions and dimensions of GO

Items	Carbon (%)	Oxygen (%)	Lateral size (μm)	Thickness (nm)
Value range	46–60	40–54	0.5–3	~1.0

values of UHPC with the MSF content of 0.5, 1.0, and 1.5% at 56 days are 119, 128, and 139 MPa, respectively, which represent an increase of 13.8, 4.0, and 2.0%. It also suggests that the compressive strength is enhanced with the increase in MSF content for a given age and GO dosage.

The compressive strength tested at 7, 28, and 56 days under steam curing is shown in Figure 6. It is clear that the compressive strength is generally greater than that of the reference specimen for a given MSF content. It can also be seen that the compressive strength is enhanced as the content of GO is increased from 0.0 to 0.02% and then reduced as the content of GO ranged from 0.02 to 0.03% at all tested ages, again supporting an optimal dosage of GO of around 0.02%. The compressive strength of the specimen with a 0.02% of GO and incorporating 0.5, 1.0, and 1.5% of MSF at 56 days is 137, 149, and 158 MPa, respectively, which represents an increase of 2.2, 6.4, and 3.0%, indicating that the compressive

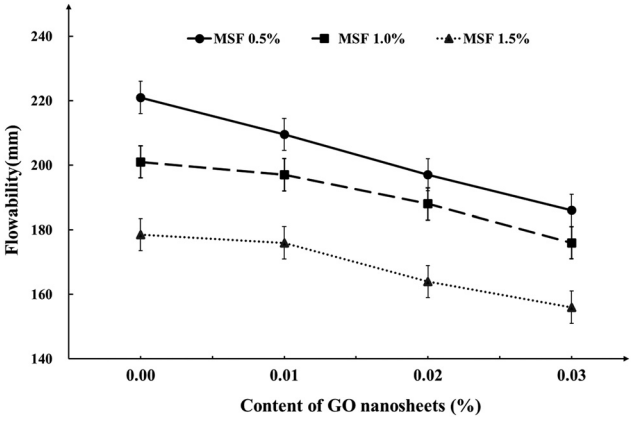

Figure 4: Flowability of fresh mixtures.

strength is enhanced with the increase in MSF content for a given age and GO dosage.

Generally, the results gained from both the curing processes have confirmed that the incorporation of GO can marginally improve the compressive strength of UHPC for a given MSF content. It is also notable that its optimal dosage under both curing regimes is around 0.02%, while the compressive strength is enhanced with the increase in MSF content for a given age and GO dosage. The improvement in compressive strength may be associated with the incorporation of both GO and MSF. The former may promote cement hydration, refine pore structure, encourage compact microstructure, and improve interfacial bond with the matrix [49]. Increase in the MSF content should decrease the space between MSF and provide more MSF to transmit load, thereby improving the compressive strength [5].

3.4 Flexural strength of UHPC influenced by GO

The flexural strength tested at 7, 28, and 56 days under standard curing is shown in Figure 7. It is observed that for a given MSF content and age, the flexural strength is significantly improved following the incorporation of GO. The trend of flexural strength at 7 and 28 days varies, but for all specimens it becomes similar at 56 days with the flexural strength enhanced as the content of GO is increased from 0.0 to 0.02% and then decreases from 0.02 to 0.03%, indicating an optimal dosage under standard curing is in the order 0.02%. The flexural strength of UHPC with 0.5% of MSF and incorporating 0.01, 0.02, and 0.03% of GO at 56 days is 26.1, 34.9, and 26.4 MPa, an increase of 2.4, 37.7, and 4.2%, respectively, while the flexural strength of UHPC with 1.0% of MSF and containing the same GO at 56 days is 32.4, 43.3, and 40.3 MPa, an increase of 9.6, 47.0, and 36.8%, respectively, compared to the reference specimen. For the specimen with a 1.5% of MSF, the flexural strength of UHPC incorporating a 0.01, 0.02, and 0.03% of GO at 56 days is 44.7, 48.6, and 46.2 MPa, an increase of 21.9, 32.4, and 25.8%, respectively. It is therefore demonstrated that the flexural strength of UHPC is significantly improved by incorporating GO under standard curing.

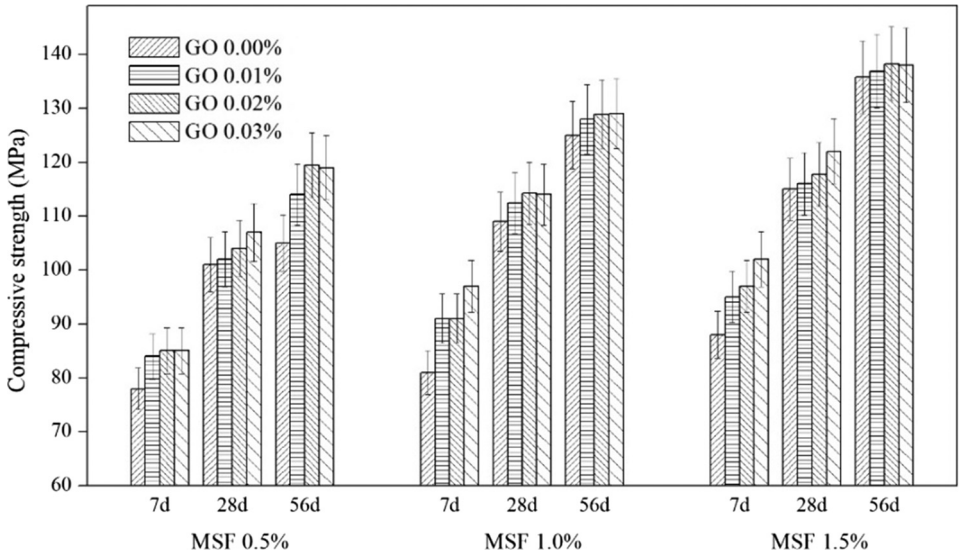

Figure 5: Compressive strength of UHPC under standard curing.

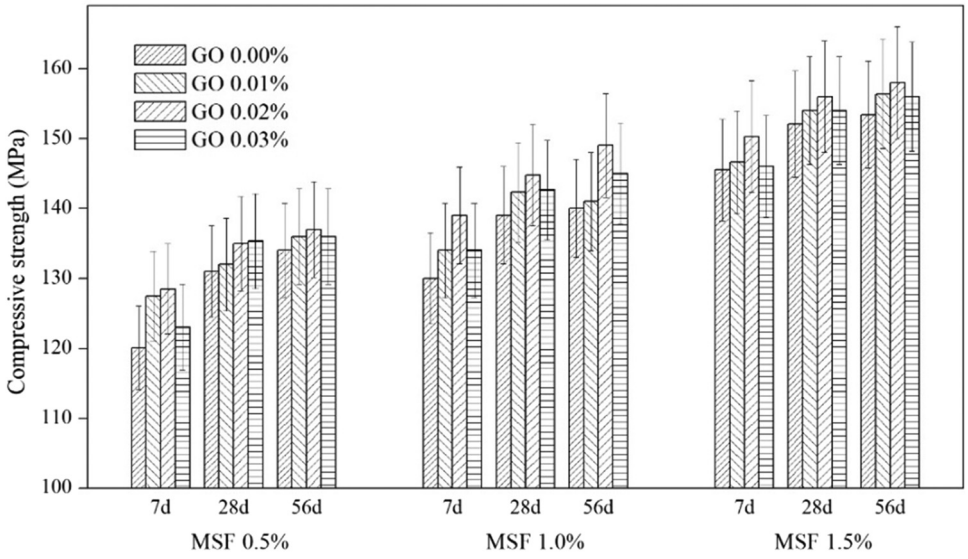

Figure 6: Compressive strength of UHPC under steam curing.

The flexural strength of UHPC tested at ages of 7, 28, and 56 days under steam curing is shown in Figure 8. It is apparent that for a given MSF and age, the flexural strength of UHPC with GO is greatly enhanced when the content of GO is added from 0.0 to 0.02% and then decreased from 0.02 to 0.03%, suggesting the optimal dosage of GO is in the order of 0.02%. At 56 days, the flexural strength of UHPC with 0.5% of MSF and containing 0.01, 0.02, and 0.03% of GO is 30.5, 33.5, and 31.6 MPa, respectively, representing an increase of 2.7, 12.6, and 6.37%, while the flexural strength for UHPC with 1.0% of MSF and corresponding GO is 42.0, 45.9, and 42.7 MPa, respectively, representing an increase of 5.5, 15.3, and 7.4% compared to the control concrete. It is also observed at 56 days that the flexural strength of UHPC with 1.5% of MSF and 0.01, 0.02, and 0.03% of GO is 51.1, 62.5, and 53.5 MPa, respectively, representing an increase of 24.9, 52.4, and 30.5%. It is therefore evident that the flexural strength of UHPC with the addition of GO is significantly improved under such curing.

The results gained from both the standard curing and steam curing have confirmed that the flexural strength has been significantly improved. As previously discussed, this might be associated with the promotion of cement

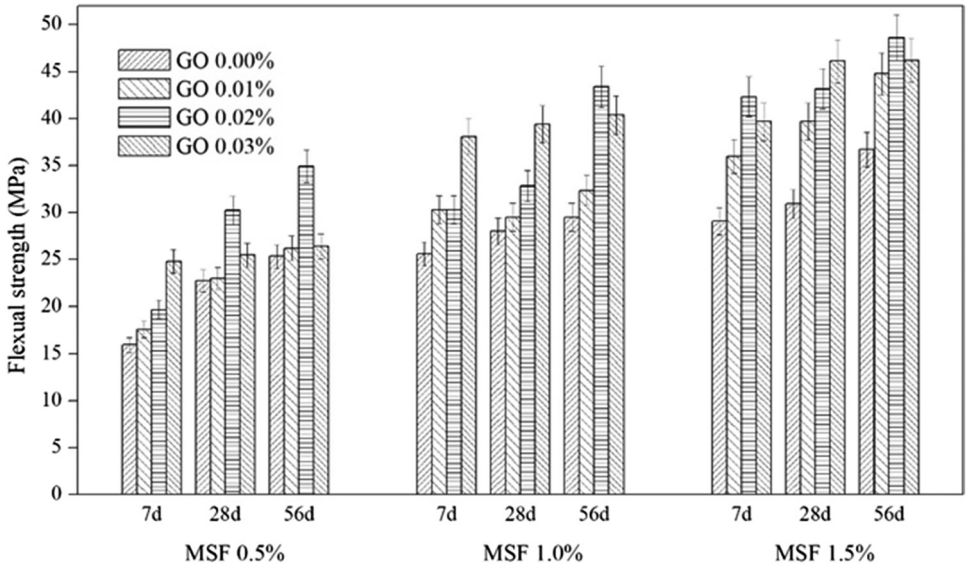

Figure 7: Flexural strength of UHPC under standard curing.

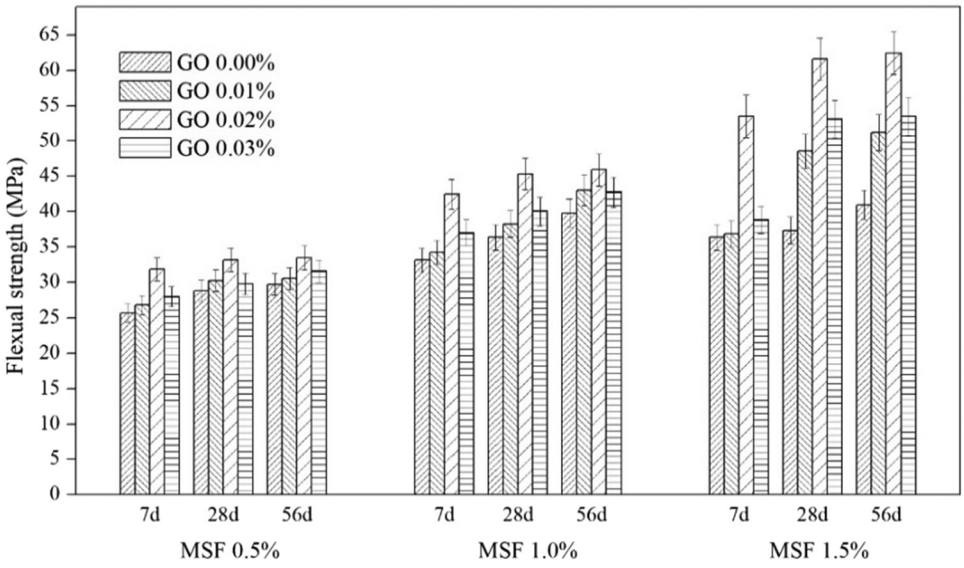

Figure 8: Flexural strength of UHPC under steam curing.

hydration, a more refined pore structure and compacted microstructure, and interfacial bond with the matrix as a result of the addition of GO [49]. It could also be attributed to the incorporation of MSF with its increase in content reducing the space between the MSFs and providing more MSF to sustain load, leading to the enhancement of flexural strength [5]; however, further discussion in present study will be carried out on the basis of the results obtained from the fiber pull-out test.

As referred previously, as the dosage of GO is added from 0.02 to 0.03% the compressive strength under steam curing and flexural strength under both standard curing and steam curing increase up to 0.02% of additions before dropping but remains greater than that of the reference specimen. This decrease in trend could be due to the higher dosage of GO failing to be uniformly dispersed [50].

Table 4 summarizes the improvement in the compressive and flexural strengths of UHPC obtained from previous studies and present work. It is observed that all the compressive strengths of UHPC is enhanced slightly, while flexural strength is improved significantly. It is also apparent that the increase in flexural strength of UHPC containing GO ranges from 39.7 to 65.0%, which supports the addition of GO as one possible measure to improve the flexural strength of UHPC.

Table 4: Improvement in compressive and flexural strengths of UHPC*

Refs.	w/c	MSF (%)	Measures employed	Curing regime	Compressive strength increase (%) (days)	Flexural strength increase (%) (days)
[12]	0.23	2	CRSM	Lime water	4.8/28 days	42.0/28 days
[13]	0.2	2	LSDCFFM	Steam curing	11.0/NA	33.0/NA
	0.22	2			8.0/NA	35.0/NA
[18,51]	0.2	0.5	CNF (0.3%)	Steam curing	3.4/28 days	45.7/28 days
			GNPC (0.3%)		4.5/28 days	59.2/28 days
			GNPM (0.3%)		4.0/28 days	38.9/28 days
Present study	0.18	1.5	GO (0.02%)	Standard curing	2.4/28 days	39.7/28 days
			GO (0.03%)		6.1/28 days	49.3/28 days
			GO (0.02%)	Steam curing	2.6/28 days	65.0/28 days
			GO (0.03%)		1.3/28 days	42.2/28 days

*CRSM: controlling rheology of suspending mortar; LSDCFFM: L-shape device to control the flow of fresh mixture; CNF: carbon nanofiber; GNPC: graphite nanoplatelets (2–10 nm × 25 mm); GNPM: graphite nanoplatelets (2–10 nm × 30 mm); Lime water: lime saturated water at room temperature; NA: not available.

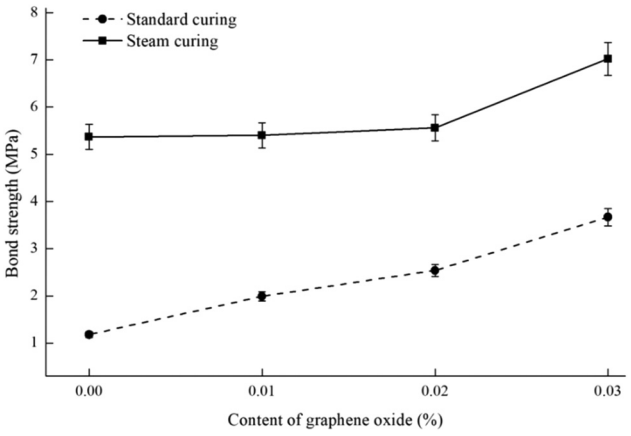

Figure 9: Bond strength between a single fiber and the bulk matrix of UHPC at 7 days.

3.5 Bond strength between single steel fiber and the bulk matrix of UHPC

Bond strength between a single steel fiber and the bulk matrix of UHPC at 7 days is shown in Figure 9. It can be seen that the incorporation of GO improves the bond strength under both standard curing and steam curing. For specimens containing the GO content of 0.0, 0.01, 0.02, and 0.03% under standard curing, the corresponding bond strength is 1.2, 2.0, 2.5, and 3.7 MPa, respectively. For specimens with GO additions of 0.01, 0.02, and 0.03% under steam curing, the bond strength is increased by 1.0, 4, and 31%, respectively, compared to the one without containing GO. It is also apparent that the bond strength of the specimen incorporating similar dosage of GO under steam curing is much greater than that of the specimens under standard curing. This is associated with the effect of the steam curing in promoting the pozzolanic reactivity [16].

3.6 Discussion on the effects of GO on microstructure and mechanical performances of UHPC

As presented in Sections 3.3 and 3.4, the addition of GO has a slight enhancement on the compressive strength of

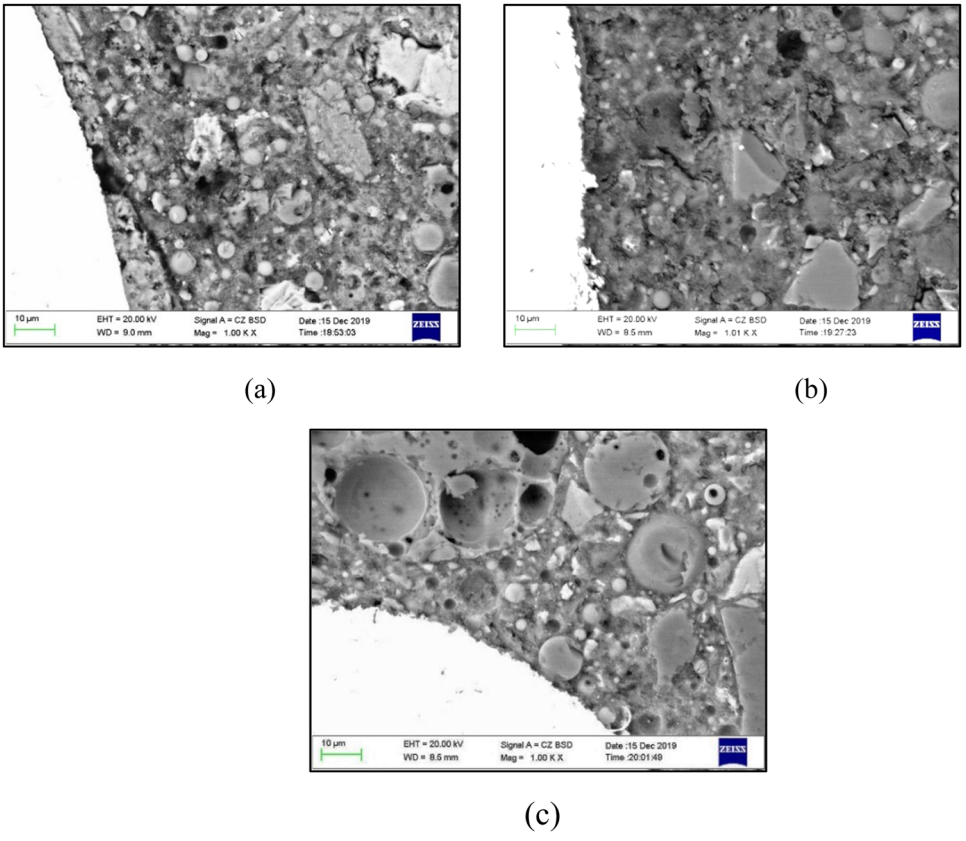

Figure 10: BSE image of interface between a fiber and the bulk matrix at 7 days: (a) referenced specimen without GO; (b) specimen with 0.02% of GO under standard curing; and (c) specimen with 0.2% of GO under steam curing.

the UHPC. It is important to be noted that its flexural strength is improved significantly by containing GO. As illustrated in Figure10, the microstructure of the matrix of the UHPC containing GO shows no significant difference from that without GO. This may be the reason why the compressive strength of UHPC with GO was not enhanced to a notable extent. In comparison, the bond strength between fiber and the UHPC matrix usually plays a greater role in the improvement of flexural strength than that on compressive strength. As described in the Section 3.5, the bond strength between fiber and the UHPC matrix is increased as the content of GO ranges from 0.01 to 0.03%, thereby leading to a higher flexural strength than that without GO.

A recent study on the effect of GO on single fiber bond behavior within mortar also indicated that the addition of GO can improve the bond between fiber and mortar matrix, where it was suggested that the enhanced compressive strength of mortar helps create better interface bonds [52]. Elsewhere, it was attributed to the higher friction increase and mechanical interlock at the interface between the steel fiber and the bulk matrix, thanks to the addition of GO [38]. In the present study, the microstructure of the interface between fiber and the matrix was characterized by means of SEM examination. As illustrated in Figure 10, it is observed that the microstructure of the interface between the fiber and the matrix of the UHPC with GO shows no significant difference from that without GO, indicating that the enhancement of bond strength by GO not only may be due to the improvement in interfacial microstructure, but also can be contributed to the higher friction increase and mechanical interlock as aforementioned, which is subjected to be further investigated.

4 Conclusion

The work presented in this study leads to the following conclusions:

(1) The EC method to synthesize GO is safer, greener, and of lower cost. It is therefore considered suitable for fabricating GO for cement paste, mortar, normal concrete, high-performance concrete, and UHPC for construction industry.
(2) The addition of GO provides a slight enhancement from 1.3 to 6.1% on the compressive strength of UHPC under both standard curing and steam curing.
(3) The findings show that the flexural strength of UHPC is significantly increased by 33 to 65% when GO is added to the mixture of UHPC under both standard curing and steam curing, demonstrating that the incorporation of GO can be an effective measure to improve the flexural strength of UHPC.
(4) The improvement of bond strength between the MSFs and the matrix can be contributed to the improved interfacial microstructure, the higher friction increase, and the mechanical interlock at the interface between the MSFs and the bulk matrix, thanks to the addition of GO.

Funding information: This study was funded by National Natural Science Foundation of China (Grant number: 50978058), Foshan University, China (Grant number: GG040995), and GT New Materials and Infrastructure Technology Ltd, China (Grant number: GTRD201901).

Author contributions: All authors have accepted responsibility for the entire content of this manuscript and approved its submission.

Conflict of interest: David Hui, who is the co-author of this article, is a current Editorial Board member of *Nanotechnology Reviews*. This fact did not affect the peer-review process. The authors declare no other conflict of interest.

References

[1] De Larrard F, Sedran T. Optimization of ultra-high-performance concrete by the use of a packing model. Cem Concr Res. 1994;24:997–1009.
[2] FerrieraL E, Michel L, Zuber B, Chanvillard G. Mechanical behaviour of ultra-high-performance short-fibre-reinforced concrete beams with internal fibre reinforced polymer bars. Compos Part B. 2015;68:246–58.
[3] Meng W, Khayat KH. Effect of graphite nanoplatelets and carbon nanofibers on rheology, hydration, shrinkage, mechanical properties, and microstructure of UHPC. Cem Concr Res. 2018;105:64–71.
[4] Hannawi K, Bian H, Prince-Agbodjan W, Raghavan B. Effect of different types of fibers on the microstructure and the mechanical behavior of ultra-high performance fiber-reinforced concretes. Compos Part B. 2016;86:214–20.
[5] Wu Z, Shi C, He W, Wu L. Effects of steel fiber content and shape on mechanical properties of ultra high performance concrete. Constr Build Mater. 2016;103:8–14.
[6] Sovják R, Shanbhag D, Konrád P, Zatloukal J. Response of thin UHPFRC targets with various fibre volume fractions to deformable projectile impact. Procedia Eng. 2017;193:3–10.
[7] Abrishambaf A, Pimentel M, Nunes S. Influence of fibre orientation on the tensile behaviour of ultra-high performance

fibre reinforced cementitious composites. Cem Concr Res. 2017;97:28–40.
[8] Zhou Z, Qiao P. Tensile behavior of ultra-high performance concrete: analytical model and experimental validation. Constr Build Mater. 2019;201:842–51.
[9] Shaikh FUA, Luhar S, Arel HS, Luhar I. Performance evaluation of ultrahigh performance fibre reinforced concrete – a review. Constr Build Mater. 2020;232:117152.
[10] Xue J, Briseghella B, Huang F, Nuti C, Tabatabai H, Chen B. Review of ultra-high performance concrete and its application in bridge engineering. Constr Build Mater. 2020;260:119844.
[11] Song Q, Yu R, Shui Z, Wang X, Rao S, Lin Z, et al. Key parameters in optimizing fibres orientation and distribution for ultra-high performance fibre reinforced concrete (UHPFRC). Constr Build Mater. 2018;188:17–27.
[12] Meng W, Khayat KH. Improving flexural performance of ultra-high-performance concrete by rheology control of suspending mortar. Compos Part B. 2017;117:26–34.
[13] Huang H, Gao X, Li L, Wang H. Improvement effect of steel fiber orientation control on mechanical performance of UHPC. Constr Build Mater. 2018;188:709–21.
[14] Nazar S, Yang J, Thomas BS, Azim I, Rehman SKU. Rheological properties of cementitious composites with and without nanomaterials: A comprehensive review. J Clean Prod. 2020;272:122701.
[15] Song H, Li X. An overview on the rheology, mechanical properties, durability, 3D printing, and microstructural performance of nanomaterials in cementitious composites. Materials. 2021;14(11):2950.
[16] Wu Z, Khayat KH, Shi C. Nano-SiO_2 particles and curing time on development of fiber-matrix bond properties and microstructure of ultra-high strength concrete. Cem Concr Res. 2017;25:247–56.
[17] Wille K, Loh KJ. Nanoengineering ultra-high-performance concrete with multiwalled carbon nanotubes. J Transp Res Board. 2010;2142:119–26.
[18] Meng W, Khayat KH. Mechanical properties of ultra-high-performance concrete enhanced with graphite nanoplatelets and carbon nanofibers. Compos Part B. 2016;107:113–22.
[19] Makar JM, Chan GW. Growth of cement hydration products on single-walled carbon nanotubes. J Am Ceram Soc. 2009;92(6):1303–10.
[20] Alatawna A, Birenboim M, Nadiv R, Buzaglo M, Peretz-Damari S, Peled A, et al. The effect of compatibility and dimensionality of carbon nanofillers on cement composites. Constr Build Mater. 2020;232:117–41.
[21] Shamsaei E, de Souza FB, Yao X, Benhelal E, Akbari A, Duan WH. Graphene-based nanosheets for stronger and more durable concrete: a review. Constr Build Mater. 2018;183:642–60.
[22] Liu C, Huang X, Wu Y-Y, Deng X, Zheng Z, Xu Z, et al. Advance on the dispersion treatment of graphene oxide and the graphene oxide modified cement-based materials. Nanotechnol Rev. 2021;10(1):34–49.
[23] Liu C, Huang X, Wu Y-Y, Deng X, Liu J, Zheng Z, et al. Review on the research progress of cement-based and geopolymer materials modified by graphene and graphene oxide. Nanotechnol Rev. 2020;9(1):155–69.
[24] Wang M, Yao H. Comparison study on the adsorption behavior of chemically functionalized graphene oxide and graphene oxide on cement. Materials. 2020;13(15):3274.
[25] Wang Y, Yang J, Ouyang D. Effect of graphene oxide on mechanical properties of cement mortar and its strengthening mechanism. Materials. 2019;12(22):3753.
[26] Mohammed A, Sanjayan JG, Duan WH, Nazari A. Incorporating graphene oxide in cement composites: a study of transport properties. Constr Build Mater. 2015;84:341–7.
[27] Liu C, Huang X, Wu Y-Y, Deng X, Zheng Z. The effect of graphene oxide on the mechanical properties, impermeability and corrosion resistance of cement mortar containing mineral admixtures. Constr Build Mater. 2021;288:123059.
[28] Wu Y-Y, Que L, Cui Z, Lambert P. Physical properties of concrete containing graphene oxide nanosheets. Materials. 2019;12:1707.
[29] Devi SC, Khan RA. Effect of graphene oxide on mechanical and durability performance of concrete. J Build Eng. 2019;27:101007.
[30] Lu L, Ouyang D. Properties of cement mortar and ultra-high strength concrete incorporating graphene oxide nanosheets. Nanomaterials. 2017;7(7):187.
[31] Shanmugavel D, Selvaraj T, Ramadoss R, Raneri S. Interaction of a viscous biopolymer from cactus extract with cement paste to produce sustainable concrete. Constr Build Mater. 2020;257:119585.
[32] Sui Y, Liu S, Ou C, Liu Q, Meng G. Experimental investigation for the influence of graphene oxide on properties of the cement-waste concrete powder composite. Constr Build Mater. 2021;276:122229.
[33] Liu C, Huang X, Wu Y-Y, Deng X, Liu J, Zheng Z, et al. Review on the research progress of cement-based and geopolymer materials modified by graphene and graphene oxide. Nanotechnol Rev. 2020;9(1):155–69.
[34] Liu C, He X, Deng X, Wu Y-Y, Zheng Z, Liu J, et al. Application of nanomaterials in ultra-high performance concrete: a review. Nanotechnol Rev. 2020;9(1):1427–44.
[35] Liu C, Huang X, Wu Y-Y, Deng X, Zheng Z. The effect of graphene oxide on the mechanical properties, impermeability and corrosion resistance of cement mortar containing mineral admixtures. Constr Build Mater. 2021;288:123059.
[36] Jiang W, Li X, Lv Y, Zhou M, Liu Z, Ren Z, et al. Cement-based materials containing graphene oxide and polyvinyl alcohol fiber: mechanical properties, durability, and microstructure. Nanomaterials. 2018;8(9):638.
[37] Yao X, Shamsaei E, Chen S, Zhang QH, de Souza FB, Sagoe-Crentsil K, et al. Graphene oxide-coated Poly(vinyl alcohol) fibers for enhanced fiber-reinforced cementitious composites. Compos Part B. 2018;174:107010.
[38] Lu Z, Yao J, Leung CKY. Using graphene oxide to strengthen the bond between PE fiber and matrix to improve the strain hardening behavior of SHCC. Cem Concr Res. 2019;126:105899.
[39] Wu Y-Y, Zhang J, Liu CJ, Zheng Z, Lambert P. Effect of graphene oxide nanosheets on physical properties of ultra-high-performance concrete with high volume supplementary cementitious materials. Materials. 2020;13:1929.
[40] Yu L, Wu R. Using graphene oxide to improve the properties of ultra-high-performance concrete with fine recycled aggregate. Constr Build Mater. 2020;259:120657.

[41] Pei S, Wei Q, Huang K, Cheng H-M, Ren W. Green synthesis of graphene oxide by seconds timescale water electrolytic oxidation. Nat Commun. 2018;9:145.
[42] Hummers WS, Offerman RE. Preparation of graphitic oxide. J Am Chem Soc. 1959;80:1339–9.
[43] Marcano DC, Kosynkin D, Berlin JM, Sinitskii A, Sun Z, Slesarev A, et al. Improved synthesis of graphene oxide. ACS Nano. 2010;4:4806–14.
[44] Chinese National Standards. GB/T175-2007, Chinese cement: common portland cement. Beijing, China: Chinese National Standards; 2007 (In Chinese).
[45] Huang ZY, Cao FL. Effects of nano-materials on the performance of UHPC. Mater Rev. 2012;26(9):136–41 (in Chinese).
[46] ASTM C1437 – 15. Standard test method for flow of hydraulic cement mortar. West Conshohocken, PA, USA: ASTM International; 2015.
[47] BS EN 196-1:2016. Methods of testing cement – part 1: determination of strength. London, UK: British Standards Institution; 2016.
[48] CECS 13. Standard test method for fiber reinforced concrete. Beijing, China: Chinese National Standards; 2009 (In Chinese).
[49] Zhao L, Guo X, Song L, Song Y, Dai G, Liu J. An intensive review on the role of graphene oxide in cement-based materials. Constr Build Mater. 2020;241:117939.
[50] Gao Y, Jing HW, Chen SJ, Du MR, Chen WQ, Duan WH. Influence of ultrasonication on the dispersion and enhancing effect of graphene oxide–carbon nanotube hybrid nanoreinforcement in cementitious composite. Compos Part B. 2019;164:45–53.
[51] Meng W, Khayat KH. Effect of graphite nanoplatelets and carbon nanofibers on rheology, hydration, shrinkage, mechanical properties, and microstructure of UHPC. Cem Concr Res. 2018;105:64–71.
[52] Chindaprasirt P, Sukontasukkul P, Techaphatthanakon A, Kongtun S, Ruttanapun C, Yoo D, et al. Effect of graphene oxide on single fiber pullout behavior. Constr Build Mater. 2021;280:122539.